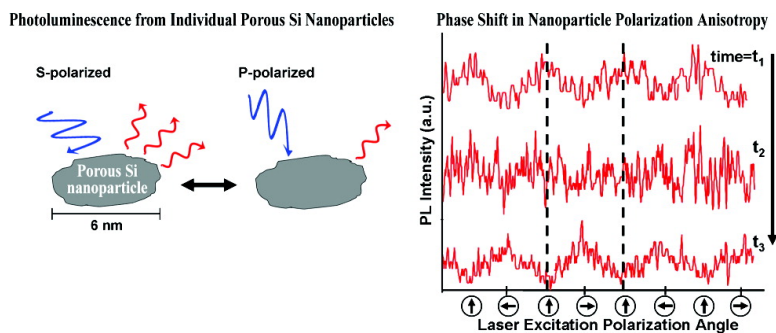# Optical Anisotropy in Individual Porous Silicon Nanoparticles Containing Multiple Chromophores

Donald J. Sirbuly, Daniel J. Gargas, Michael D. Mason, Paul J. Carson, and Steven K. Buratto

More About This Article

Additional resources and features associated with this article are available within the HTML version:

- Supporting Information
- Links to the 1 articles that cite this article, as of the time of this article download
- Access to high resolution figures
- Links to articles and content related to this article
- Copyright permission to reproduce figures and/or text from this article

View the Full Text HTML

Optical Anisotropy in Individual Porous Silicon Nanoparticles Containing Multiple Chromophores

Donald J. Sirbuly,[†] Daniel J. Gargas, Michael D. Mason,[‡] Paul J. Carson, and Steven K. Buratto*

Department of Chemistry and Biochemistry, University of California, Santa Barbara, California 93106. [†]Current address: Chemistry, Materials, and Life Sciences Directorate, Lawrence Livermore National Laboratory, Livermore, CA 94550. [‡]Current address: Department of Chemical and Biological Engineering, University of Maine, Orono, ME 04469.

ABSTRACT Polarization anisotropy is investigated in single porous silicon nanoparticles containing multiple chromophores. Two classes of nanoparticles, low current density and high current density, are studied. Low current density samples exhibit red-shifted spectra and contain only one or two chromophores. High current density particles, on average, contain less than four chromophores and display a blue-shifted spectrum. We utilize single-molecule spectroscopy to probe the polarization effects of the particles, and we show that both classes of particles are influenced by a polarized excitation source. These results are exciting at the fundamental level for understanding coupled quantum dot emitters as well as for applications involving single-photon sources or silicon-based polarization-sensitive detectors.

KEYWORDS: porous Si · silicon nanocrystals · single-molecule fluorescence · polarization anisotropy

Visible light emission from anodically etched silicon, also known as porous silicon (PSi), continues to interest researchers due to its trivial synthetic preparation and unique optical properties. Since its discovery in 1990,[1] there has been an ongoing motivation to understand the luminescence mechanism in the material.[2–6] One of the important components to understanding the photoluminescence is how polarized excitation affects the emissive states. Previous reports have shown that bulk PSi displays a large degree of absorbance sensitivity when excited with linearly polarized light.[7–13] This can be partially explained by the anisotropic etching (*i.e.*, Si pillar formation) of the silicon wafer under anodic potentials.[5,14] Since the electrochemical etching produces low-dimensional wire-like silicon structures (generally parallel to the [100] axis), it is reasonable to assume that the luminescence intensity of the PSi will be stronger when the excitation polarization is aligned with the major axis of the Si wires.

These observations in bulk PSi can be further explained using a dielectric model.[9,10] Here PSi is treated as a series of dielectric ellipsoids embedded in an effective dielectric medium, where the major axes of the ellipses are aligned along the [100] direction. More recently, a theoretical study on the polarization effects in PSi described how the photoluminescence anisotropy arises due to optical transitions in an asymmetric silicon crystal.[15] The optical transitions are calculated using a tight-binding technique and interpreted through an effective mass theory. Interestingly, the size of the ac-

tive silicon crystal can greatly affect the orientation of the dipole moment. Being that silicon is an indirect band gap semiconductor, conservation of momentum occurs through the absorption or emission of a crystal vibration mode (*i.e.*, a phonon). In general, as the crystal becomes more confined, the uncertainty in the crystal momentum increases.[3] This translates into an increase in zero-phonon transitions as the size of the nanocrystal decreases.[3,16] In this article, we experimentally investigate single nanoparticles of PSi, containing different-sized active regions (*i.e.*, chromophores), and probe the polarization effects as the excitation vector is rotated in real time.

RESULTS AND DISCUSSION

Our experimental approach to studying the polarization anisotropy in PSi involves removing the Si chromophore from the bulk and applying single-molecule spectroscopic techniques.[17–20] The fluorescence spectra in Figure 1A represent two classes of PSi nanoparticles. The HCD sample was etched at 20 mA for 10 min, whereas the LCD sample was etched at 5 mA for 10 min.
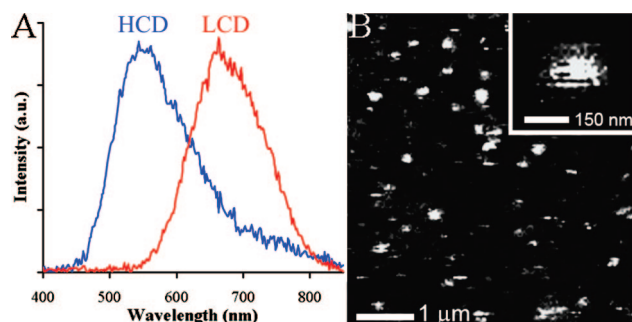
Figure 1. Photoluminescence spectra and confocal fluorescence image of PSi nanoparticles dispersed on glass. **(A)** Each spectrum represents an average of ~10 single particle spectra (10 s integration time), under 457 nm CW excitation. Nanoparticles prepared under low current density (LCD) exhibit a fluorescence maximum (λ_{max} = 675 nm) significantly red-shifted from that of high current density (HCD) particles (λ_{max} = 550 nm). **(B)** A typical confocal fluorescence image of individual PSi nanoparticles on glass. The bright spots represent the particles on a linear gray scale (white ~20 kcps). Inset shows a zoomed-in region of a single PSi nanoparticle.

Each spectrum was obtained by integrating over several scan lines in a typical 15 × 15 μm fluorescence image and represents ~10 nanoparticles. The large blue shift in the HCD sample can be explained by an excited-state confinement effect.[21,22] At higher current density, the resulting porous silicon framework is extremely fragile, due to the smaller silicon nanostructures. In previous work, we showed that our HCD samples undergo a severe internal collapse of the silicon network after the solvent evaporates.[23] This result can be explained by the three-dimensional etching that takes place under the HCD conditions. The opposite is true for the LCD case. The porous film remains attached to the silicon substrate after evaporation of the solvent, indicative of a larger, more rigid silicon framework. This is largely due to an anisotropic etch (two-dimensional) that dominates in the formation of the porous medium under LCD conditions.

Before probing the effects of polarization modulation, it is crucial to know the number of emitting centers in each individual PSi nanoparticle and understand
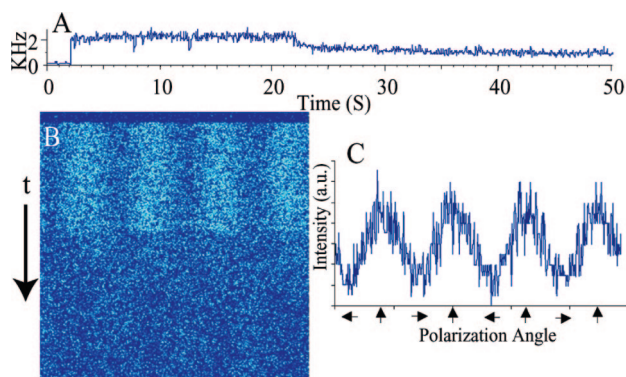

Figure 2. Polarization data taken from a LCD nanoparticle. **(A)** Intensity trajectory of a single LCD nanoparticle. The data is binned by 125 ms (equal to a single scan line). Background signal is ~1 kcps. **(B)** Unbinned time course image as linearly polarized light is rotated 720° per scan line. **(C)** Plot of the fluorescence intensity *versus* polarization angle. Data averaged over the "on" time.

how the size of the particle relates to chromophore size. In earlier experiments, we determined that the average particle size for both LCD and HCD was 6 nm, with 95% of the particles falling in the range of 4.5–8 nm. According to previous theoretical work, visible luminescence from quantum-confined silicon should occur only at diameters <4 nm.[24] This suggests that the active silicon chromophore must represent a small portion of the silicon crystallite. Since the HCD etching conditions produce a smaller silicon grain (blue-shifted luminescence), it makes sense that a HCD PSi particle would contain more chromophores. We determined the number of chromophores in both LCD and HCD samples by employing a single-particle statistical method.[25] In both cases, the nanoparticles contain more than one chromophore. In the LCD samples, ~70% of the measured nanoparticles contain only a singe emitting center, whereas in the HCD sample, fewer than half of the particles measured contain a single emitting chromophore, and a significant percentage contain three or four chromophores.

The fluorescence image in Figure 1B illustrates a typical 15 × 15 μm scan of PSi nanoparticles dispersed on a glass coverslip under an inert atmosphere. After parking the excitation beam over a single particle, the luminescence can be monitored as a function of polarization angle. Figure 2A captures a typical polarization intensity time course of a single LCD nanoparticle. The image in Figure 2B displays the unbinned data as the polarized excitation is rotated 720° per line. The sinusoidal pattern in Figure 2C is the result of collapsing the "on" time counts of the particle onto the fast time axis (*x*-axis). The intensity level reaches the background signal (~1 kilocount per second (kcps)) at the trough of the wave, suggesting that the absorption cross-section of the emitting chromophore(s) approaches zero at this point. It is unclear, in this case, if multiple chromophores are emitting. However, considering the laser power at the sample (~125 W/cm²), the intensity level during the "on" time (1 kcps), and the agreement with previous studies under similar conditions, we would conclude that only one chromophore is emitting with a strong polarization anisotropy.

Treating the chromophores as elliptical crystallites supports the observed time course for the LCD nanoparticles. Since the etching process forms vertical pillars of silicon along the [100] planes, it is expected that the chromophores are also aligned along this axis plane. Therefore, an enhancement in the fluorescence signal should be observed when the excitation polarization is parallel to the growth axis. The data in Figure 2 that shows a single, strong polarization anisotropy represents the majority of the traces captured on the LCD nanoparticles, which correlates well with previous reports.[26] This also agrees with our previous findings that the LCD particles generally contain only one chromophore. However, as Figure 3 illustrates, there are par-
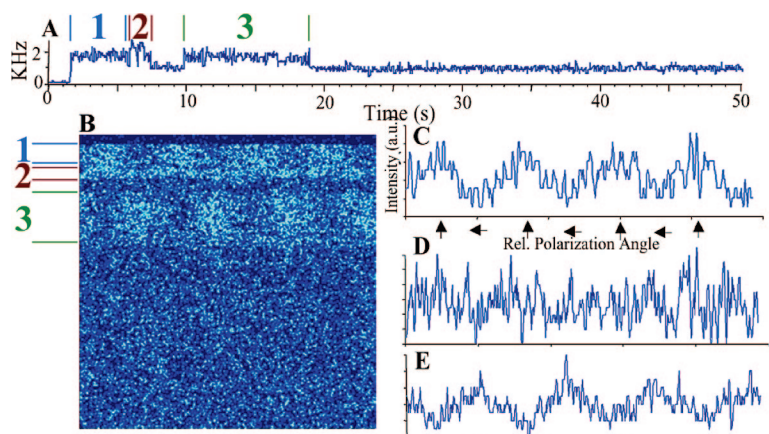
Figure 3. Polarization data taken from a LCD nanoparticle. (A) Intensity trajectory of a single LCD nanoparticle. The data is binned by 125 ms. Background signal is ~1 kcps. (B) Unbinned time course image as linearly polarized light is rotated 720° per scan line. (C−E) Data averaged over regions 1 (C), 2 (D), and 3 (E).

pole oriented 90° to the initial emitting chromophore. With opposing dipoles, the polarization anisotropy is canceled out and appears as a flat trace in Figure 3D. After both chromophores blink off, only the chromophore oriented 90° to the first chromophore turns back on, leaving a 90° phase-shifted profile. The second explanation involves the same scenario as above through region 2, but in region 3 a third chromophore turns on with a 90° dipole orientation relative to the first chromophore. Last, it is possible that two different chromophores with opposing dipole

ticles generated from LCD etching conditions that show multiple-chromophore behavior.

The intensity trajectory in Figure 3A shows three "on" regions labeled 1, 2, and 3. Ordinarily this time course would be treated as a PSi particle entering a "dark" state, blinking on again, and then remaining off for the rest of the trace. With randomly or circularly polarized light, it would be impossible to state whether the "on" regions are due to the same chromophore, multiple emitters, or a different chromophore turning on. However, as linearly polarized light is rotated during the time course (Figure 3B), a clear distinction is observed. In region 1, a strong polarization anisotropy is captured (Figure 3C), but region 2 shows a washing out of the polarization (Figure 3D), with a slight increase in the overall fluorescence intensity (Figure 3A). After the particle enters a dark state and blinks on again, there is a 90° phase shift in the polarization trace (Figure 3E). The data can be interpreted one of three ways. First, a second chromophore turns on in region 2 that has a di-

orientations turn on in region 2 at the same time the first chromophore blinks off. After all chromophores turn off, only one chromophore turns back in region 3. With any of these scenarios, the data supports a system containing multiple chromophores (most likely two) that are aligned with their long axes perpendicular to each other. It is important to note that a majority (~70%) of the data collected thus far on the LCD nanoparticles show strong polarization anisotropy similar to Figure 2, whereas <5% display a response similar to Figure 3.

The HCD nanoparticles, which contain a larger number of chromophores, should display polarization effects similar to anomalies observed in the LCD particles (Figure 3). Figure 4 is a representative data series for a HCD sample probed under conditions similar to those used for the LCD nanoparticles. The time course in Figure 4A displays multiple levels, and the unbinned time course image (Figure 4B) shows a strong anisotropic polarization. The first 12 s of the time course has an inten-
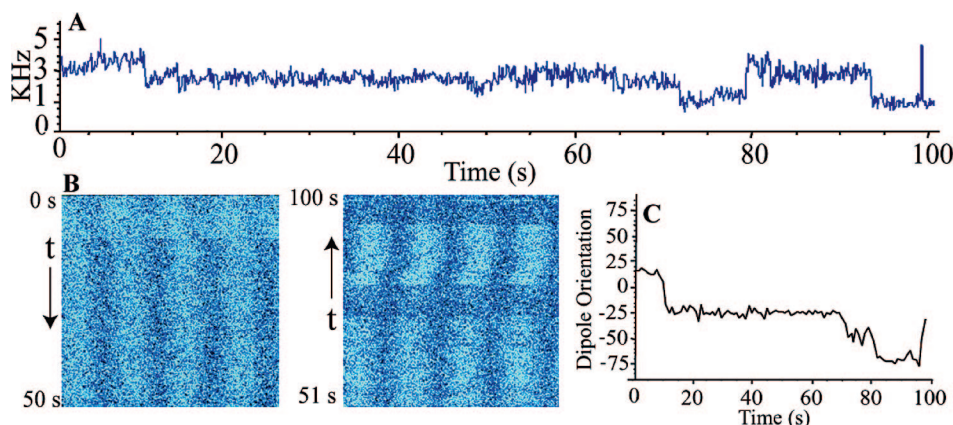

Figure 4. Polarization data from a HCD nanoparticle. (A) Intensity trajectory of a single HCD PSi nanoparticle. Background signal is ~1 kcps. (B) Unbinned time course images as linearly polarized light is rotated four times per line trace. The first image (time axis downward) is for the first 50 s of the time course. The second image (time axis upward) is for the last 50 s of the time course. (C) Plot showing the excited-state dipole orientation *versus* time during the course of the intensity trajectory. Dipole orientation (angle) is referenced to the initial orientation (at time = 0) only. The dipole orientation is undefined during "off" times.

sity level 3 times that of the ~1 kcps background, suggesting that at least three chromophores are emitting simultaneously. From the time course image in Figure 4B, it is apparent that there is a small net dipole in the particle during this time, which changes to a strong polarization anisotropy, slightly shifted (~40°), starting at 12 s and ending at 72 s. After a long "off" time, the particle blinks on with a slightly phase-shifted signal. At time equal to 83 s, the dipole rotates during the "on" period 33°, which is better illustrated in the dipole orientation plot (Figure 4C). The exact orientation of the particle and chromophore under the microscope is arbitrary, but the plot shows the relative dipole movement in real time. The progression of the dipole orientation is on a much slower time scale than the frequency generator, ruling out a simultaneous dipole and polarization vector movement. If the modulation was due to the function generator shifting its phase, the oscillating signal would broaden due to the short pixel dwell time of ~195 μs/data point. To verify a stagnant waveform, the function generator was constantly monitored using a synchronous output to the waveform. The sync signal showed negligible phase-walking during the time span of the experiments.

The explanation of polarization results for the initial 12 s is similar to that of the multichromophore LCD nanoparticles. The intensity level suggests that at least three chromophores are emitting. With a larger number of randomly oriented dipoles, the scrambled polarization anisotropy in the first 12 s is expected. As the time course persists, one or two chromophores turn off at the 12 s mark and leave two or one, respectively, still emitting. All chromophores turn off at 72 s, but multiple chromophores begin re-emitting photons at *ca.* 79 s. Interestingly, once the chromophores turn on, a strong polarization signal persists with an intensity level suggesting at least three chromophores are emitting. During this "on" time, a mechanism differing from the LCD case could help explain the wandering anisotropic signature. This model allows multiple chromophores to emit with different orientations but still give an overall dipole across the entire nanoparticle. If one of the chromophores ionizes (ejects an electron from the Si crystal), due to an Auger-type ionization process,[19,27,28] there would be an induced dipole (charge separation) across the nanoparticle which could lead to a strong polarization axis. The data does not support three chromophores turning on simultaneously with aligned dipoles due to the multiple polarization states seen in the dipole orientation plot. In addition, it would be very unlikely for the dipole orientation to exhibit real-time drift (*i.e.*, not have discrete states) if individual chromophores were simply turning on and off. This behavior has never been observed in LCD nanoparticles and provides an ideal platform for studying coupled quantum dot systems.
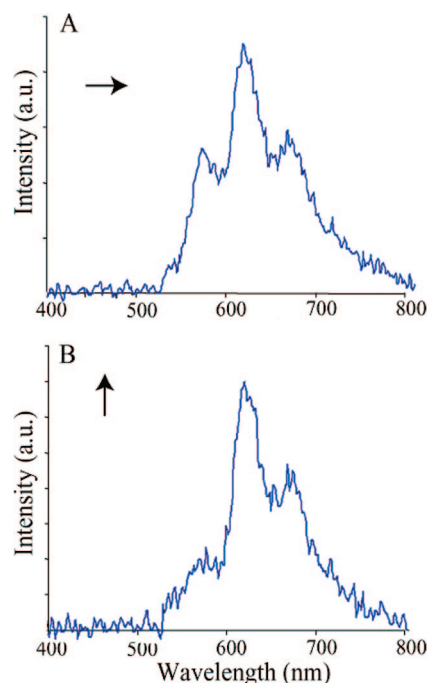

Figure 5. Spectra of a single PSi nanoparticle showing spectral splitting at two different linear polarization angles. Polarization direction (black arrows) is only relative to the other.

The fluorescence spectra of PSi nanoparticles can also be a valid means of understanding polarization effects in low-dimensional materials. The emission spectra of bulk and nanoparticle PSi is generally broad (fwhm > 200 nm) and featureless. However, the luminescence spectrum of individual nanoparticles often displays vibronic structure similar to that shown in Figure 5. The peak splitting is believed to be a result of vibronic coupling to Si$-$O modes of the particle that arise within the passivating layer on the surface of the Si nanoparticle. The effects of the surface passivating layer, a mixture of Si, O, and H of varying stoichiometry, on the luminescence from porous Si have been discussed thoroughly by Gole and co-workers.[31-33] The measured splitting in the spectra of Figure 5 is ~ 1300 cm^{-1} (~ 160 meV) which is consistent with the Si$=$O stretch of oxide-passivated silicon (1100–1300 cm^{-1}) observed by Gole *et al.*[31] As depicted in Figure 5, the higher energy peak diminishes relative to the other peak as the excitation is rotated 90°. This decrease in intensity could be due to a single, higher frequency emitting chromophore that has its long axis aligned perpendicular to the electric field vector. As expected, the vibronic coupling remains strong as the polarized excitation is rotated, but the absorption cross-section of the chromophore decreases, causing a weaker emission. The other emitting chromophore(s) likely has a weak dipole or its long axis is oriented 45° relative to the polarization axis.

In conclusion, we have determined that multiple emitting centers exist in individual PSi nanoparticles

prepared from electrochemically etched bulk samples. They can be treated as small segments of the bulk crystalline material. Particles generated from low current densities exhibit a red-shifted spectrum and contain on average only one or two chromophores. Nanoparticles prepared under high current density conditions contain ≤4 emitting chromophores and have a spectral blue shift. Strong polarization anisotropy is observed in both LCD and HCD nanoparticles. The data support the model that most of the chromophores formed during the etching process are elliptical in shape. In the HCD nanoparticles, there is a larger distribution of randomly oriented chromophores, assumed to be due to the three-dimensional etching at high current densities. In the LCD case, a two-dimensional etch dominates, producing chromophores aligned predominantly along the [100] crystal direction. Chromophores emitting simultaneously can display a net zero dipole, but these events occur more abundantly in a HCD particle. In addition, dipole wandering was observed only in the HCD nanoparticles. We proposed that this real-time dipole reorientation is caused by an ionized chromophore inducing charge separation across the particle. After the charged chromophore is thermally neutralized, the particle returns to a stable polarization state. These findings demonstrate a novel means of studying coupled quantum dot emitters and provide a unique system for understanding light production from silicon-based optical materials.

METHODS

Porous silicon nanoparticles were prepared using a method similar to that described by Heinrich et al.[20] Briefly, a p-type [100] Si wafer was anodically etched in a 15% hydrofluoric acid/10% hydrogen peroxide/ethanol electrolyte. Red- and green-emitting samples were prepared by etching for 10 min at 5 mA/cm^2 (low current density, LCD) and for 10 min at 20 mA/cm^2 (high current density, HCD), respectively.[23] After etching, the PSi film was mechanically removed into chloroform and diluted to 1 nM. All colloid solutions were sonicated for 24 h to reduce particle size and eliminate aggregates. The nanoparticles were spatially isolated by spin-casting a 30 μL aliquot of the 1 nM colloid solution onto a clean glass coverslip.

Fluorescence from single nanoparticles was detected and imaged using a laser scanning confocal microscope (LSCM) equipped with a high numerical aperture oil-immersion objective (Zeiss, 1.3 NA).[29] After spinning the PSi particles on a glass coverslip, the sample was inverted and placed on a home-built variable ambient scanning stage.[30] The sample chamber was evacuated, back-filled with nitrogen, and kept at a constant flow rate during the experiment. The 457 nm line of an Ar^+ (Spectra-Physics), attenuated to ~125 W/cm^2, was used to excite the sample. The beam was focused through the cover glass to a nearly diffraction-limited spot at the nitrogen/glass interface. A beam splitter was placed in the path of the fluorescence to allow both images (Digital Instruments) and spectra (Princeton Applied Research) to be acquired. Fluorescence intensity trajectories were captured by parking the excitation spot over a single nanoparticle and monitoring the luminescence intensity as a function of time. Linearly polarized light was rotated using a simple optical train consisting of an electro-optic modulator (Fastpulse Technology) and a λ/4 waveplate. A function generator applied a ramping voltage to the EOM with a frequency matched to the scanning electronics.

REFERENCES AND NOTES

1. Canham, L. T. Silicon Quantum Wire Array Fabrication by Electrochemical and Chemical Dissolution of Wafers. *Appl. Phys. Lett.* **1990**, *57*, 1046–1048.
2. Brus, L. Luminescence of Silicon Materials—Chains, Sheets, Nanocrystals, Nanowires, Microcrystals, and Porous Silicon. *J. Phys. Chem.* **1994**, *98*, 3575–3581.
3. Hybertsen, M. S. Absorption and Emission of Light in Nanoscale Silicon Structures. *Phys. Rev. Lett.* **1994**, *72*, 1514–1517.
4. Prokes, S. M. Study of the Luminescence Mechanism in Porous Silicon Structures. *J. Appl. Phys.* **1993**, *73*, 407–413.
5. Cullis, A. G.; Canham, L. T.; Calcott, P. D. J. The Structural and Luminescence Properties of Porous Silicon. *J. Appl. Phys.* **1997**, *82*, 909–965.
6. Collins, R. T.; Fauchet, P. M.; Tischler, M. A. Porous Silicon: From Luminescence to LEDs. *Phys. Today* **1997**, *50*, 24–31.
7. Zheng, W. H.; Xia, J. B.; Cheah, K. W. Linear Polarization of Photoluminescence in Quantum Wires. *J. Phys: Condens. Matter* **1997**, *9*, 5105–5116.
8. Efros, A. L.; Rosen, M.; Averboukh, B.; Kovalev, D.; BenChorin, M.; Koch, F. Nonlinear Optical Effects in Porous Silicon: Photoluminescence Saturation and Optically Induced Polarization Anisotropy. *Phys. Rev. B* **1997**, *56*, 3875–3884.
9. Lavallard, P.; Suris, R. A. Polarized Photoluminescence of an Assembly of Non Cubic Microcrystals in a Dielectric Matrix. *Solid State Commun.* **1995**, *95*, 267–269.
10. Kovalev, D.; Benchorin, M.; Diener, J.; Koch, F.; Efros, A. L.; Rosen, M.; Gippius, N. A.; Tikhodeev, S. G. Porous Si Anisotropy from Photoluminescence Polarization. *Appl. Phys. Lett.* **1995**, *67*, 1585–1587.
11. Andrianov, A. V.; Kovalev, D. I.; Zinovev, N. N.; Yaroshetskii, I. D. Anomalous Photoluminescence Polarization of Porous Silicon. *JETP Lett.* **1993**, *58*, 427–430.
12. Starukhin, A. N.; Lebedev, A. A.; Razbirin, B. S.; Kapitonova, L. M. Hidden Anisotropy of Emitting Transitions in Porous Silicon. *Pis'ma Zh. Tekhnich. Fiz.* **1992**, *18*, 60–63.
13. Koyama, H. Strong Photoluminescence Anisotropy in Porous Silicon Layers Prepared by Polarized-Light Assisted Anodization. *Solid State Commun.* **2006**, *138*, 567–570.
14. Herino, R.; Perio, A.; Barla, K.; Bomchil, G. Microstructure of Porous Silicon and its Evolution with Temperature. *Mater. Lett.* **1984**, *2*, 519–523.
15. Allan, G.; Delerue, C.; Niquet, Y. M. Luminescence Polarization of Silicon Nanocrystals. *Phys. Rev. B* **2001**, *63*, 205301–8.
16. Kovalev, D.; Heckler, H.; Ben-Chorin, M.; Polisski, G.; Schwartzkopff, M.; Koch, F. Breakdown of the k-Conservation Rule in Si Nanocrystals. *Phys. Rev. Lett.* **1998**, *81*, 2803–2806.
17. Balagurov, L. A.; Yarkin, D. G.; Petrovicheva, G. A.; Petrova, E. A.; Orlov, A. F.; Andryushin, S. Y. Highly Sensitive Porous Silicon Based Photodiode Structures. *J. Appl. Phys.* **1997**, *82*, 4647–4650.
18. Betzig, E.; Finn, P. L.; Weiner, J. S. Combined Shear Force and Near-Field Scanning Optical Microscopy. *Appl. Phys. Lett.* **1992**, *60*, 2484–2486.
19. Mason, M. D.; Credo, G. M.; Weston, K. D.; Buratto, S. K. Luminescence of Individual Porous Si Chromophores. *Phys. Rev. Lett.* **1998**, *80*, 5405–5408.
20. Heinrich, J. L.; Curtis, C. L.; Credo, G. M.; Kavanagh, K. L.; Sailor, M. J. Luminescent Colloidal Silicon Suspensions from Porous Silicon. *Science* **1992**, *255*, 66–68.

21. Fauchet, P. M.; vonBehren, J. The Strong Visible Luminescence in Porous Silicon: Quantum Confinement, Not Oxide-Related Defects. *Phys. Status Solidi B: Basic Res.* **1997**, *204*, R7–R8.

22. Lehmann, V.; Gosele, U. Porous Silicon Formation - A Quantum Wire Effect. *Appl. Phys. Lett.* **1991**, *58*, 856–858.

23. Mason, M. D.; Sirbuly, D. J.; Buratto, S. K. Correlation Between Bulk Morphology and Luminescence in Porous Silicon Investigated By Pore Collapse Resulting from Drying. *Thin Solid Films* **2000**, *406*, 151–158.

24. Delley, B.; Steigmeier, E. F. Size Dependence of Band-Gaps in Silicon Nanostructures. *Appl. Phys. Lett.* **1995**, *67*, 2370–2372.

25. Mason, M. D.; Sirbuly, D. J.; Carson, P. J.; Buratto, S. K. Investigating Individual Chromopores Within Single Porous Silicon Nanoparticles. *J. Chem. Phys.* **2001**, *114*, 8119–8123.

26. Koyama, H. Different Behavior Of Photoluminescence Anisotropy in Porous Silicon Layers Made by Polarized-Light-Assisted Electrochemical Etching. *Appl. Phys. Lett.* **2002**, *80*, 965–967.

27. Empedocles, S. A.; Norris, D. J.; Bawendi, M. G. Photoluminescence Spectroscopy of Single CdSe Nanocrystallite Quantum Dots. *Phys. Rev. Lett.* **1996**, *77*, 3873–3876.

28. Kovalev, D.; Heckler, H.; Ben-Chorin, M.; Polisski, G.; Schwartzkopff, M.; Koch, F. Auger Processes in the Ensemble of Si Nanocrystals. *J. Porous Mater.* **2000**, *7*, 85–91.

29. Weston, K. D.; Buratto, S. K. Millisecond Intensity Fluctuations of Single Molecules at Room Temperature. *J. Phys. Chem. A* **1998**, *102*, 3635–3638.

30. Sirbuly, D. J.; Schmidt, J. P.; Mason, M. D.; Summers, M. A.; Buratto, S. K. Variable-Ambient Scanning Stage for a Laser Scanning Confocal Microscope. *Rev. Sci. Instrum.* **2003**, *74*, 4366–4368.

31. Gole, J. L.; Prokes, S. M. Resonantly Excited Photoluminescence from Porous Silicon and the Question of Bulk Phonon Replicates. *Phys. Rev. B* **1998**, *58*, 4761–4770.

32. Dixon, D. A.; Gole, J. L. Potential Role of Silanone and Silylenes in the Photoluminescence-Excitation, Visible-Photoluminescence-Emission and Infrared Spectra of Porous Silicon. *Phys. Rev. B* **1998**, *57*, 12002–12016.

33. Gole, J. L.; Veje, E.; Egeberg, R. G.; Ferreira da Silva, A.; Pepe, I.; Dixon, D. A. Optical Anlysis of the Light Emission from Porous Silicon: A Hybrid Polyatom Surface-Coupled Fluorophore. *J. Phys. Chem. B* **2006**, *110*, 2064–2073.